^{4}He interaction with and scattering from graphite

N. García
Departamento de Física Fundamental, Universidad Autonoma de Madrid, Canto Blanco, Madrid, Spain

William E. Carlos* and Milton W. Cole
Department of Physics, The Pennsylvania State University, University Park, Pennsylvania 16802

V. Celli
Department of Physics, University of Virginia, Charlottesville, Virginia 22901
(Received 19 March 1979; revised manuscript received 29 May 1979)

Calculations are presented of diffraction intensities for the scattering of ^{4}He from graphite basal plane. The potential employed is a corrugated hard wall plus attraction. The choice of parameters is made by modeling a more realistic potential derived by pairwise summation of He-C interactions. These pair interactions are taken to be of either Yukawa-6 or Lennard-Jones 6-12 form, with coefficients derived by comparison with experimental data of Boato *et al.* (differing in value from those used traditionally). The computed linewidths, positions, and splittings are in good overall agreement with the scattering results. The role of inelastic effects is explored using a complex potential with a constant imaginary part for small atom-surface separation.

I. INTRODUCTION

Recent advances in the analysis of scattering of monoenergetic beams of light atoms from crystals have made this a valuable technique for studying surfaces.[1] This paper makes use of data obtained in recent experiments[2-4] on ^{4}He scattering from the basal (1000) plane of graphite to elucidate the nature of the He graphite interaction potential $V(\vec{r})$. The potential-energy function is an essential ingredient for understanding the intriguing properties of ^{4}He and ^{3}He films adsorbed on graphite.[5-7] Moreover, the determination of $V(\vec{r})$ permits one to appraise calculated forms of the potential.[5] Since $V(\vec{r})$ depends on the electronic properties of the surface, information about the latter can be gleaned from this analysis.

A variety of potentials will be discussed in this paper and therefore it is important to establish their interrelation. The scattering calculation will be performed with a model potential

$$V(\vec{r}) = \infty, \quad z < \zeta(\vec{R}), \tag{1a}$$

$$V(\vec{r}) = -D, \quad \zeta(\vec{R}) < z < \beta, \tag{1b}$$

$$V(\vec{r}) = V_a(z), \quad z > \beta. \tag{1c}$$

Here $\vec{r} = (\vec{R}, z)$ is the atomic position and z the coordinate normal to the surface. This potential represents a corrugated hard wall, bounded by the surface $z = \zeta(\vec{R})$, which has the periodicity of the graphite basal plane, shown in Fig. 1. The function $V_a(z)$ represents a long-range van der Waals attraction; its form is discussed in Sec. III.

Such a corrugated hard wall plus long-range attraction has been used previously to treat He scattering from alkali-halide surfaces.[1,2,8-10] The values of D and the functions $\zeta(\vec{R})$ and $V_a(z)$ are chosen by comparison with more realistic potentials discussed in Sec. III. Although the model form (1) is adopted primarily for computational convenience, it does incorporate the qualitative behavior of a real potential. In particular, Eq. (1) is capable of yielding rather good agreement with the bound state resonances, the band-structure splittings[11,12] and the diffraction intensities observed experimentally.[2-4,13] In fact, as we shall show in Sec. III, both the realistic potentials and the model Eq. (1) are capable of revealing inconsistencies in the preliminary experimental data (especially weakly bound states and behavior near threshold[13-15]).

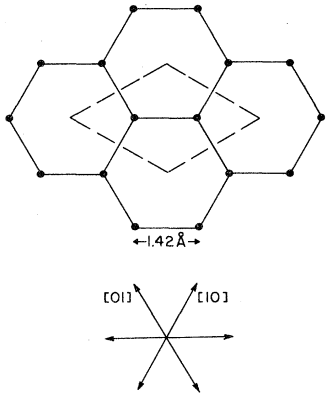

FIG. 1. Hexagonal symmetry of the graphite lattice, showing rhombic unit cell. Carbon atoms lie at the vertices. Also shown are the six smallest nonzero reciprocal-lattice vectors.

This paper is organized as follows. Section II presents the method[10] used to calculate the diffraction intensity for the model potential (1). Section III discusses more realistic potentials, based on *ab initio* calculations or on the assumption that $V(\vec{r})$ can be written as a pairwise sum of He–C interactions:

$$V(\vec{r}) = \sum_i U(\vec{r} - \vec{R}_i), \tag{2}$$

where $\vec{R}_i$ is the equilibrium position of the ith C atom. This form was assumed by Chow[16] in a recent calculation of He scattering from graphite. Both the latter calculation and many previous ones assumed a pair potential which is rather inconsistent with the subsequent experimental data.[2-4] Section IV presents the results for the diffractive scattering intensity and provides a detailed analysis of lineshapes, resonance widths, and splittings. Our conclusions are presented in Sec. V.

II. SOLUTION OF THE SCATTERING PROBLEM

Since Ref. 10 reports the technique used here for determining the diffractive scattering intensity we restrict the present discussion to a summary of the relevant results. With the Rayleigh hypothesis,[17-20] the incident wave (modified by the attractive potential) can be evaluated at the corrugated hard wall[10]:

$$\psi_i(\vec{R}, \zeta(\vec{R})) = \sum_{\vec{G}} B_{\vec{G}} e^{i(\vec{K}+\vec{G})\cdot\vec{R}} \times [e^{ik'_{\vec{G}z}\zeta(\vec{R})} + R(k^i_{\vec{G}z}) e^{-ik'_{\vec{G}z}\zeta(\vec{R})}]. \tag{3}$$

The summation is over the set of two-dimensional reciprocal-lattice vectors $\vec{G}$. The incident wave vector $\vec{k} = (\vec{K}, -k_{\vec{0}z})$, has a projection $\vec{K}$ on the surface plane. The periodic corrugation couples $\vec{K}$ to the set of vectors

$$\vec{K}' = \vec{K} + \vec{G}. \tag{4}$$

The wave vector $k'_{\vec{G}z}$ depends on the strength of the attractive potential:

$$k'^2_{\vec{G}z} = k^2_{\vec{G}z} + 2mD/\hbar^2, \tag{5a}$$

$$k^2_{\vec{G}z} = k^2 - (\vec{K} + \vec{G})^2. \tag{5b}$$

In Eq. (3), the coefficients $R(k'_{\vec{G}z})$ denote the reflection coefficients[10] for a wave incident (from $z < \beta$) upon the attractive potential $V_a(z)$ of Eq. (1). The coefficents $B_{\vec{G}}$ are obtained using the procedure of Ref. 10 and the *GR* numerical method.[8] These are directly related[10] to the scattering amplitudes $A_{\vec{G}}$ for various diffraction channels:

$$e^{i\phi} A_{\vec{G}} = (k'_{\vec{G}z}/k_{\vec{G}z})^{1/2} [1 - |R(k'_{\vec{G}z})|^2]^{1/2} / [1 + R(k^i_{\vec{G}z})] \times B_{\vec{G}} - R^*(k^i_{\vec{0}z}) \delta_{\vec{G},0}, \tag{6}$$

where R^* is the amplitude of the specularly reflected wave in the potential $V_a(z)$. Knowledge of the phase factor ϕ is not necessary because the intensity of diffraction to a final state $\vec{K}' = \vec{K} + \vec{G}$ is given by

$$P_{\vec{G}} = (k_{\vec{G}z}/k_{\vec{0}z}) |A_{\vec{G}}|^2. \tag{7}$$

Because flux is conserved, the sum of $P_{\vec{G}}$ over the open channels ($k^2_{\vec{G}z} > 0$) is one, within numerical accuracy.

Garcia, Celli, and Goodman[10] have used this method successfully to treat He scattering from LiF. Since the corrugation of the hard wall is found here to be smaller for the graphite case than for LiF, we expect the Rayleigh method to work well here.[17-19]

We note in passing that the present method[10] can be generalized to the case of a variable potential in the region $\zeta(\vec{R}) < z < \beta$. Such a computation is worth performing after more experimental data become available. Alternatively, an "exact" calculation could be used combining a hard wall with more general attractive potential.[9]

III. CHOICE OF POTENTIAL $V(\vec{r})$

Several options are possible for choosing the well depth D, corrugation function $\zeta(\vec{R})$, and long range attraction $V_a(z)$ specified in Eq. (1). One such procedure is based on the assumption of a pairwise sum potential[4,5] [Eq. (2)], using a judicious choice of pair potential $U(\vec{r})$. This method is described in Sec. III A. An alternative approach is to model the result of an *ab initio* calculation of $V(\vec{r})$ performed by Freeman.[21] As discussed in Sec. III B, this potential is not sufficiently realistic to warrant its use in the scattering calculation.

Before presenting a discussion of specific alternative potentials, we should comment on their relation to the bound state resonance values ϵ_n. Because the potential $V(\vec{r})$ is periodic with respect to translation parallel to the crystal surface, it can be written in the form

$$V(\vec{r}) = \sum_{\vec{G}} V_{\vec{G}}(z) \exp(i\vec{G}\cdot\vec{R}), \tag{8}$$

where $\vec{G}$ is a two-dimensional reciprocal lattice vector appropriate to the graphite symmetry. The term $V_0(z)$, corresponding to $\vec{G} = 0$, is the lateral average of $V(\vec{r})$. To lowest approximation,[1,9-12] the observed levels ϵ_n are eigenvalues of the Schrödinger equation for a ^{4}He atom in the potential $V_0(z)$. Thus their experimental deter-

mination imposes a restriction on the parameters entering any assumed form of $V(\vec{r})$. We utilize this in the discussion of $V(\vec{r})$ below.

The data of Boato, Cantini, and Tatarek[2] were interpreted as indicating the presence of four bound states for ^{4}He on graphite. The eigenvalues ϵ_n are presented in Table I. Their results for specular scattering intensity as a function of incident angle show other minima, which were attributed to "threshold" resonances (labeled by a T in the figure). Our preliminary study, however, suggested[13] that at least one additional bound state should be present, at $\epsilon_4 \cong -0.3$ meV. Furthermore, scattering calculations[15,16,22] of the behavior near threshold imply that a jump in intensity is expected there, rather than a minimum. These arguments, supported by further results below, indicate that a reinterpretation of the data is plausible. Very recently, results confirming this hypothesis have been obtained by Derry *et al.*[3] and by Boato *et al.*[4] A small disagreement with the previous work[2] can be attributed[23] to a minute error in the experimental determination of scattering angle.

We address next the problem of choosing a model potential function for the scattering calculation by considering more realistic potentials.

A. Pairwise sum potentials

It is frequently assumed[1,5,17] that $V(\vec{r})$ can be written in the form of Eq. (2), i.e., as a sum of interactions $U(\vec{r}-\vec{R}_i)$ between the adatom at $\vec{r}$ and the substrate atoms at $\{\vec{R}_i\}$. Implicit in this assumption is the neglect of many-body interactions and any displacement of the substrate atoms from their equilibrium positions. The latter could be included by averaging over the atom's motion, but this motion is temperature dependent and such a procedure is probably not justifiable in an elastic scattering theory. With these limitations in mind we address the problem of choosing an appropriate form for the pair potential.

(1) A common choice is a Lennard–Jones 6–12 interaction,

$$U(x) = 4\epsilon[(\sigma/x)^{12} - (\sigma/x)^6], \tag{9a}$$

$$x = |\vec{r} - \vec{R}_i|. \tag{9b}$$

For this potential, Fourier transformation of Eq. (2) yields[5]

$$V_0(z) = \frac{4\pi\epsilon}{A_c} \sum_{m=0}^{\infty} \left(\frac{2\sigma^{12}}{5z_m^{10}} - \frac{\sigma^6}{z_m^4} \right), \tag{10a}$$

$$z_m = z + md, \tag{10b}$$

where $A_c = 5.24$ Å^2 is the area of the surface unit cell and $d = 3.37$ Å is the spacing between basal planes of graphite. The $\vec{G} \neq 0$ Fourier components of the potential are[5]

$$V_{\vec{G}}(z) = \left(\frac{5b\sigma^{12}G^5}{1152z^5} K_5(Gz) - \frac{5b\sigma^4 G^2}{12z^2} K_2(Gz) \right) \gamma_{\vec{G}}. \tag{11}$$

Here $b = 12\pi\sigma^2\epsilon/5A_c$, K_n is a modified Bessel function, and $\gamma_{\vec{G}} = \exp(i\vec{G}\cdot\vec{R}_1) + \exp(i\vec{G}\cdot\vec{R}_2)$, where $\vec{R}_1$ and $\vec{R}_2$ are the positions of the two C atoms in a unit cell. Depending on $\vec{G}$, $\gamma_{\vec{G}} = -1$ or $+2$.

The parameters ϵ and σ are chosen by comparing the observed bound state resonances $\{\epsilon_n\}$ with the eigenvalues of the Schrödinger equation using the potential (10). We have solved this equation by the Numerov method[24] for a range of parameters ϵ and σ. Figure 2 of Ref. 13 shows the domain of parameters which yield eigenvalues which agree with the $\{\epsilon_n\}$ reported by Boato *et al.*[2] within experimental error. Optimal agreement in the least squares sense occurs for $\epsilon = 1.34$ meV, $\sigma = 2.75$ Å. Tables I and II present the resulting eigenvalues for the two isotopes of He.

We note that previous calculations[5,16,25] using this form of potential have *assumed* a value $\sigma \cong 2.98$ Å. This estimate represents the arithmetic mean of the graphite layer spacing (3.37 Å) and the He–He interaction hard core parameter. Such a high value of σ cannot yield good agree-

TABLE I. ^{4}He-graphite bound-state energies, computed with various model potentials, and the asymptotic coefficients of those potentials.

n \ ϵ_n	Experiment[a]	$\sum$ (6–12)	$\sum$ (Yukawa–6)	Modified Freeman	Flat bottom
0	−11.75 ± 0.10	−11.73	−11.76	−10.80	−11.83
1	−6.13 ± 0.10	−5.94	−6.12	−3.9	−6.10
2	−2.65 ± 0.08	−2.64	−2.64	−1.10	−2.62
3	−0.86 ± 0.03	−0.99	−0.88	−0.24	−1.02
4	unobserved	−0.29	−0.20	−0.03	−0.28
5	unobserved	−0.06	−0.02	$\sim -9.2\times10^{-4}$	−0.06
C_3 (meV Å^3)		138.0	84.0	173.0	166.0

[a] From Ref. 2, Ref. 3 reports eigenvalues approximately 2 percent higher in magnitude.

TABLE II. ^{3}He-graphite bound state energies (meV).

n \ ϵ_n	(6–12)	Yukawa–6	Modified Freeman	Flat bottom
0	−11.17	−11.24	−9.90	−10.90
1	−4.98	−5.14	−2.90	−4.87
2	−1.85	−1.79	−0.60	−1.79
3	−0.53	−0.42	−0.08	−0.44
4	−0.10	−0.05	$\sim -3.2\times10^{-3}$	−0.09
5	−0.01	$-\sim 0.002$	$\sim -1.5\times10^{-6}$	−0.01

ment with the scattering data[2,3] (which is consistent with the thermodynamic data[6,7]). The best it can do is with $\epsilon = 1.07$ meV, which yields ^{4}He bound states $|\epsilon_n| = 11.4$, 6.0, 2.85, and 1.2 meV. These do not fall within the uncertainty of the data[2] and the deviations exhibit a suspicious systematic trend (−0.3, −0.1, +0.25, +0.3 meV).

The origin of this inadequacy of the choice $\sigma = 2.98$ Å is either a violation of the combining rule or its improper application to He–graphite (e.g., takine $\sigma_{C\text{-}C} = 3.37$ Å). Experience[26] with the σ combining rule for collisions between individual atoms suggests that it works reasonably well (slightly *underestimating* the σ of the mixed system, in contrast to the present case). By elimination, we are led to suspect that one cannot apply the rule directly to the graphite case. Indeed this is not particularly surprising because the interlayer spacing is not equal to a C–C hard-core diameter, since the spacing is determine in part by the weak van der Waals attraction between layers.[27]

(2) An alternative form of pair potential is suggested by the fact that interparticle repulsive forces in the region of electronic overlap are more accurately described by exponential variation with distance than by a power law. We consider, therefore, a "Yukawa-6" pair potential:

$$U(x) = (A/x)\exp(-\alpha_1 x) - B/x^6 . \tag{12}$$

The corresponding Fourier coefficients are

$$V_0(z) = \rho\exp(-\alpha_1 z) - 3C_3 d^{-3}\zeta(4, z/d), \tag{13}$$

$$V_{\vec{G}}(z) = \left(\frac{\rho\alpha_1[1-\exp(-\alpha_1 d)]\exp[-(\alpha_1^2+G^2)^{1/2}z]}{2(\alpha_1^2+G^2)^{1/2}} - \frac{3C_3 d\,G^2}{z^2}K_2(Gz)\right)\gamma_{\vec{G}}, \tag{14}$$

$$A = A_c\alpha_1[1-\exp(-\alpha_1 d)](\rho/4\pi),$$

$$B = 3A_c d C_3/\pi.$$

Here $\zeta(4, z/d)$ is a Riemann zeta function[28]; it appears also in Eq. (10a) through the sum of z_m^{-4} terms. Note that there are three parameters appropriate to this potential, whereas the Lennard-Jones 6-12 potential has only two. A least-squares best fit to the data of Boato *et al.*[2] gives $\alpha_1 = 3.27$ Å^{-1}, $\rho = 29.4$ eV, and $C_3 = 84$ meV Å^3. The eigenvalues resulting from this choice are shown in Tables I and II and $V_0(z)$ is shown in Fig. 2.

We note in passing that we have considered also an exp-6 form of pair potential. This differs from Eq. (12) only in the absence of the x^{-1} factor in the repulsive term. Not surprisingly, the results are not qualitatively different so we do not report them here.

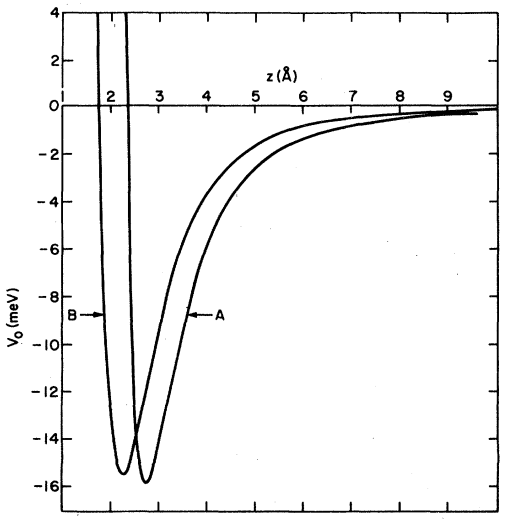

FIG. 2. The lateral average potential $V_0(z)$ for the pairwise sum of 6–12 potentials (curve A) and Yukawa-6 potentials (B).

B. *Ab initio* potential

Freeman[21] has derived a He graphite potential by a density functional method[29] which uses as input the computed[30] electronic charge density of a single layer of graphite. The result, which we call $V_F(\vec{r})$, possesses too weak an attraction (by a factor of about 2) because the method does not yield the long range van der Waals attraction. A very simplistic way to incorporate the latter is to add its known *asymptotic* form to $V_F(\vec{r})$:

$$V(\vec{r}) = V_F(\vec{r}) - C_3 z^{-3} . \tag{15}$$

The coefficient $C_3 = 173$ meV Å^3 has been computed by Watanabe[31] from the frequency dependent polarizability of He and anisotropic dielectric function of graphite. Although Eq. (15) is naive, its form is analogous to treatments of dispersion by other workers.[32] As can be seen in Tables I and II, this "modified-Freeman" potential is in fair agreement with the scattering data. One might guess that the presence of higher order terms in the

dispersion interaction might remedy the remaining deficiency. We do not know their form, however; in any case the dispersion must be modified for very small z in some unspecified way.

Although this modified-Freeman potential is of interest in the context of understanding the origin of the atom–surface interaction, it is not sufficiently accurate to justify its use in the present scattering calculation.

C. Model potential

1. Hard-wall corrugation

We choose our model potential Eq. (1) to be computationally convenient while retaining the qualitative features of the more realistic pairwise sum potentials. The hexagonal symmetry of the graphite basal plane imposes the following form on the hard-wall corrugation function:

$$\begin{aligned}\zeta(\mathrm{R}) = \zeta_0 &+ 2\zeta_1\{\cos(2\pi S_1) + \cos[2\pi(S_2 - S_1)]\} \\ &+ 2\zeta_2\{\cos[2\pi(S_1 + S_2)] + \cos[2\pi(2S_1 - S_2)] + \cos[2\pi(S_1 - 2S_2)]\} \\ &+ 2\zeta_3[\cos(4\pi S_1) + \cos(4\pi S_2) + \cos(4\pi(S_2 - S_1))] + \cdots . \end{aligned} \tag{16}$$

Here $S_1 = x/a$, $S_2 = y/a$, and $a = 2.465$ Å is the lattice constant. The coordinate system has its origin at the center of a hexagon and the x and y axes are directed toward the midpoints of a C-C bond. The Fourier amplitudes ζ_i are chosen by making reference to the pair potentials of Sec. III B. In particular, we identify the surface $z = \zeta(\vec{\mathrm{R}})$ as the locus of classical turning points for a particle of incident energy E. As can be seen in Tables III and IV, these are only weakly energy dependent because the repulsive barrier rises very steeply. For the scattering calculation we adopt the value $\zeta_1 = -0.023$ Å as an intermediate value between the low-energy results for the two potentials considered in Tables III, IV, and V. Since the higher Fourier components are an order of magnitude smaller than ζ_1, we neglect them. Furthermore, the value of ζ_0 does not affect the diffraction intensity, so we take it to be zero henceforth.

We note that the same value $\zeta_1 = -0.023$ Å was found in an eikonal analysis[2,33] of the diffraction intensity, which should be relatively accurate because of the small corrugation. An alternative procedure for generating the corrugation amplitude is to utilize[10,12] the measured band splittings.[2] Finally we mention that this He-graphite corrugation strength (crest to trough range $\Delta z = 9|\zeta_1| \simeq 0.21$ Å) is intermediate between the very smooth metal case ($\Delta z \simeq 0.1$ Å)[34] and the relatively bumpy alkali-halide case, ($\Delta z \simeq 0.6$ Å).[8]

2. Attractive well

As described in Ref. 10, a form of attractive potential which is convenient for the scattering calculation is

$$\begin{aligned} V_a(z) &= -D, \quad z < \beta, \\ V_a(z) &= -D\left(\frac{\alpha+\beta}{\alpha+z}\right)^3, \quad z \geq \beta . \end{aligned} \tag{17}$$

As can be seen from Table I, the parameters $D = 14.4$ meV, $\alpha = 1.33$ Å, and $\beta = 0.93$ Å fit the bound state resonance data quite well. The coefficient of the z^{-3} asymptotic behavior is $C_3 = D(\alpha+\beta)^3 = 166$ meV Å^3. This is closer to the theoretical value[31] of 173 meV Å^3 than either of the pairwise sum potentials, which predict 138 (84) meV Å^3 for the 6–12 (Yukawa-6) cases. Thus the large z form of $V(\vec{r})$ and weakly bound states should be more accurately described by this model potential than by the pairwise sum potentials. A possible origin of this deficiency is that a pairwise sum representation does not incorporate screening. A recent study[35] of dispersion forces for a metal indicates how screening causes the pairwise sum approximation to err at large z.

TABLE III. Values of ξ_i (Å) for the sum of 6–12 potentials.

E (meV)	ξ_0	ξ_1	ξ_2	ξ_3
20	2.229	−0.020	-7.2×10^{-4}	-1.2×10^{-3}
60	2.114	−0.021	-8.9×10^{-4}	-1.6×10^{-3}
120	2.020	−0.023	-1.2×10^{-3}	-2.0×10^{-3}

IV. DIFFRACTION INTENSITIES

Having chosen the form and parameters of the model potential, we compute intensities of the diffraction channels using the procedure of Sec. II for incident wave vector $k = 6.51$ Å^{-1}. Figure 3(a) shows the experimental data of Boato *et al.* for the specular intensity as a function of polar angle of incidence for azimuthal angle $\phi = 0$. This is to be compared with Fig. 3(b) which gives our calculation of the specular intensity. In addition Fig. 3(c) presents our calculated nonspecular diffraction intensities. The calculated and experimental specular intensities agree on all major resonance structures and the calculation for the $(0\bar{1})$ diffraction intensity agrees qualitatively with unpublished results of Boato and Cantini.[23] Because of numerical difficulties, giving rise to nonunitary results, the region near the $\epsilon_0^{(01)}$ resonance is not included in these figures.

TABLE IV. Values of ξ_i (Å) for the sum of Yukawa-6 potentials

E (meV)	ξ_0	ξ_1	ξ_2	ξ_3
20	1.624	−0.026	−0.001	−0.001
60	1.447	−0.029	−0.0015	−0.0015
120	1.286	−0.033	−0.002	−0.002

Before discussing in detail the resonance structures in the intensities we consider the reasons for the higher overall intensity in the calculated specular intensity than in the experiment. Naively one might expect the specular intensity to depend on temperature through a Debye-Waller factor (as in x-ray scattering),

$$I_{00}/I_{\text{th}} = \exp[-2W(\cos^2\theta + D/E)], \tag{18}$$

where I_{th} is the specular intensity computed for a rigid lattice (i.e., that shown in Fig. 3(b) and W is proportional to the mean square atomic displacement perpendicular to the surface.[36] The D/E term assumes that the relevant wave vector is that of the particle in the well. A fit to this form at $\theta = 30°$ yields $2W = 1.40$ when the latter correction is neglected and $2W = 0.75$ if it is included with $D = 14.4$ meV. These give very similar results; the specular intensity computed with the latter correction is shown in Fig. 4. The experimental trend shown in Fig. 3 does not agree well with this and, indeed, a simple reduction of the theoretical intensity by a factor of 1/3, independent of Θ, does better than any standard Debye-Waller correction.

Some of the disagreement between theory and experiment is due to scattering by imperfections of the graphite crystals used in the experiments, and some is due to energy broadening of the incident beam[2] ($\Delta E/E \sim 0.04$). Previous disagreement with Eq. (18) has been seen in a careful study of scattering from alkali halides.[37] While electronic excitation has been invoked to interpret the discrepancy present for scattering from a metal,[39,40] that is much less likely to explain the semimetallic graphite case. The scattering correction for thermal motion thus remains a mystery.[36]

Our calculations do describe successfully the resonance positions. It is these resonance structures in the specular intensity which are used to determine the bound-state energies. We note that unitarity is preserved by our calculation at all angles, including at resonance. That is, a minimum in the specular intensity gives rise to maximum in one of the nonspecular diffraction channels, generally one which is strongly coupled to

TABLE V. Values of ξ_i (Å) for the modified-Freeman potential.

E (meV)	ξ_0	ξ_1
20	2.320	0.018
60	2.199	0.020
120	2.101	0.022

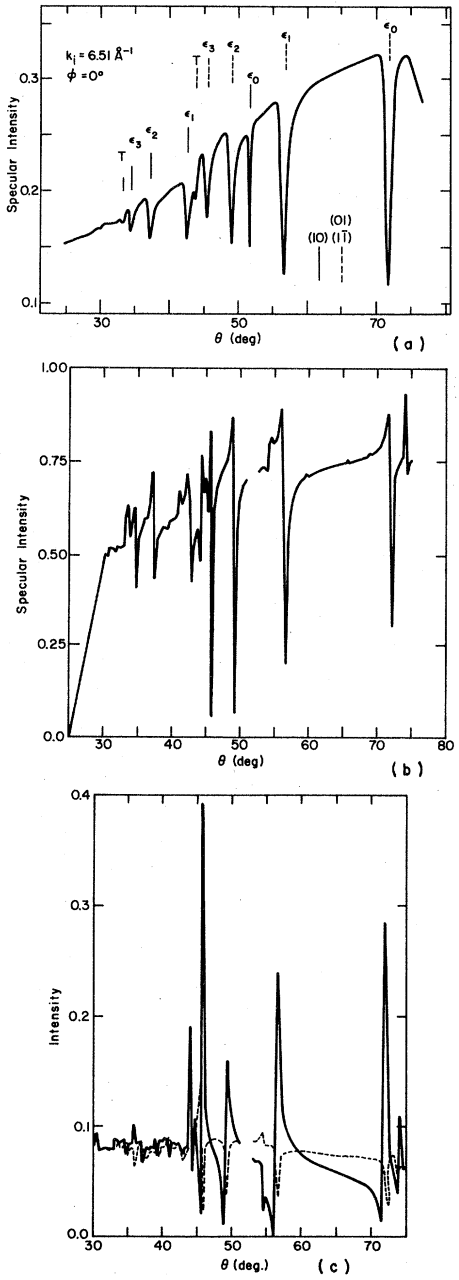

FIG. 3. Scattered beam intensities normalized to incident intensity as a function of polar angle θ for $\phi = 0$. Specular intensity measured by Boato *et al.*[2] (a) and computed (b). Part (c) shows diffracted intensity for $(\bar{1}1)$ or $(0,\bar{1})$ beams (full curve) and $(\bar{1}0)$ beam (dashed curve). (See text in relation to the omitted region.)

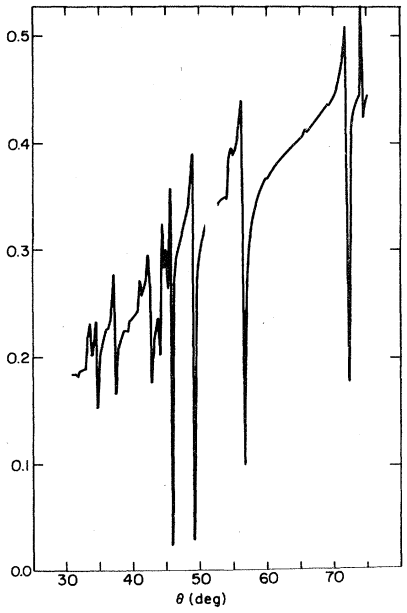

FIG. 4. Specular intensity computed with a Debye-Waller-like connection, using the well depth $D = 14.4$ meV.

the resonant state. For instance, the sharp dip in specular intensity at $\theta \simeq 72°$ is accompanied by a sharp rise in the $(\bar{1}1)$ and $(0\bar{1})$ diffraction intensities. In addition to reproducing the main features of the experimental data, our calculations also indicate much fine structure associated with resonances coupled by higher Fourier components of the potential which may become experimentally resolvable.

Reference 12 has derived an expression for the width of an isolated resonance n, corresponding to a closed-channel reciprocal-lattice vector $\vec{N}$,

$$\Gamma^n_{\vec{N}} = 2\left(\frac{d\delta}{d\epsilon}\right)^{-1}_{\epsilon_n}[1 - |S(\vec{N},\vec{N})|], \tag{19}$$

where $S(\vec{N},\vec{N})$ is the matrix element for transition from channel $\vec{N}$ to $\vec{N}$, and δ is the phase of the reflection coefficient $R(k'_{\vec{N}z})$ due to the potential $V_a(z)$, for waves incident from the left. For the corrugated hard-wall potential,[12]

$$S(\vec{F},\vec{N}) = \frac{1}{A_c}\int_{A_c} \exp\{i[\vec{R}\cdot(\vec{F}-\vec{N}) + \zeta(\vec{R})(k'_{\vec{F}z} + k'_{\vec{N}\epsilon})]\}d^2R. \tag{20}$$

This matrix element represents the eikonal approximation to the scattering matrix equation. As noted in Ref. 12, the linewidths are determined largely by $d\delta/d\epsilon$, which is inversely proportional to the semiclassical approximation to the level spacing. A more careful analysis includes the dependence on $|S(\vec{N},\vec{N})|$, which increases with quantum number. This may explain why $\Gamma^0_{(10)} < \Gamma^1_{(10)}$ [Fig. 3(a)]; other widths have the same order as the derivatives of Table VI.

A striking discrepancy between the calculations and the data of Boato *et al.*[2] is the absence of sharp structure predicted here, especially near threshold. Partly responsible is the fact that the beam is not monoenergetic and perfectly collimated. The disagreement, however, is somewhat worse than in the alkali–halide case, for which the experimental broadening factors are comparable. A possible explanation is a higher probability of inelastic losses for graphite than for alkali halides. The difference may arise from the graphite elastic anisotropy, associated with the weak interlayer binding.[41] Alternatively, the semimetallic electronic structure[30] may be responsible because of the possibility of low-energy electronic excitation[42] in the collision. The latter has been proposed[38] recently to explain data for He scattering from the (001) surface of Cu.[39,40] It would be of considerable value to explore these alternatives with *ab initio* inelastic calculations of the atom-surface interaction. Lacking such calculations, we pursue a phenomenological model of inelastic effects. Assuming the loss mechanism to be of short range,[43] we employ an optical potential form[16]

$$V_{op}(z) = V_a(z)[1 + i(D_{op}/D)\Theta(\beta - z)], \tag{21}$$

where $V_a(z)$ is given in Eq. (17) and $\Theta(\beta - z)$ is a step function. The calculation proceeds as in the elastic case, except that $k'_{\vec{G}z}$ is complex so that unitarity is not satisfied.[38] Figure 5 exhibits results for the case $D_{op} = 0.75$ meV, an arbitrary, but not unreasonable, choice.

For comparison, Fig. 5 shows also the results calculated without taking into account inelastic effects. The general shape of the computed resonance structures is much closer to those observed when inelastic effects are included. However, the positions of the resonance minima appear to be unaffected by the inclusion of inelastic effects. A more complete calculation of this effect should be performed, along with simulation and convolution of experimental broadening factors to discriminate between alternative origins of the resonance line shape.

As previously mentioned, the positions of the

TABLE VI. Values of $d\delta/d\epsilon$ for the flat-bottom potential, Eq. (17) (meV), evaluated at the bound-state energies ϵ_n.

n	0	1	2	3	4	5
$\left(\frac{d\delta}{d\epsilon}\right)^{-4}_{\epsilon=\epsilon_n}$	0.81	0.80	0.44	0.16	0.11	0.03

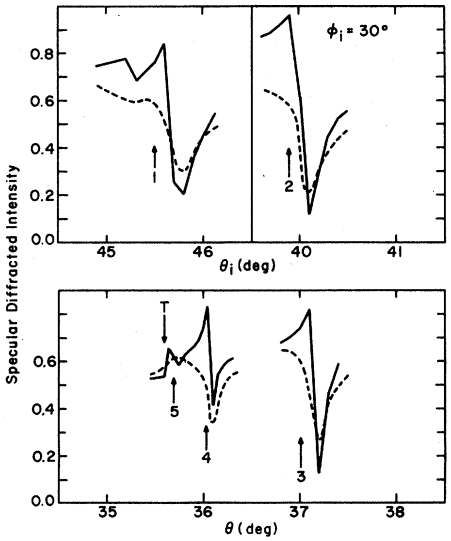

FIG. 5. Computed specular intensity showing the role of inelastic effects. Full curve employs a real potential; dashed curve uses Eq. (21). Arrows indicate positions of unperturbed levels.

resonance structures are used to determine the eigenvalues of the laterally averaged atom-surface potential. The loci of the resonances in the $\vec{K}$ plane, as observed by Boato *et al.*[2] are shown in Fig. 6. As can be seen, the resonances follow free-particle-like circles very well except in regions near degeneracies (e.g., the K_y, $\phi = 30°$, axis) where they deviate due to band structure effects. Figure 7 shows experimental data for the crossing of the 0(10) and 0(01) resonances, indicating the deviation from the free-particle positions. As noted by Chow,[16,44] a particle incident at $\phi = 30°$ couples only to the symmetric combination of the two unperturbed states. Hence

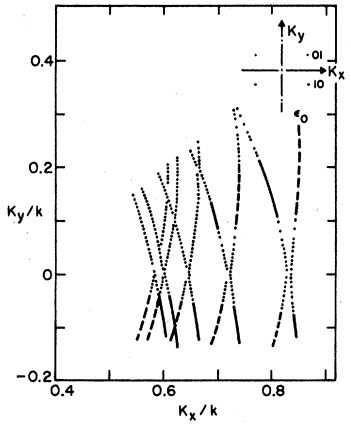

FIG. 6. Loci of the observed[23] resonance positions as a function of the projection $\vec{K}$ of the incident wave vector.

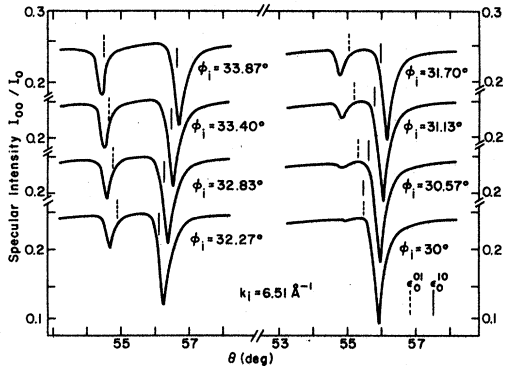

FIG. 7. Experimental data from Ref. 2 for the resonance structure near the crossing of 0(10) and 0(01) states. The unperturbed level positions are noted by vertical bars.

only one resonance is seen at $\phi = 30°$, shifted from the position expected from the free-atom circle. Our calculation for $n = 0$ is shown in Fig. 8 while those for the higher resonances are shown in Fig. 5. The experimental and calculated angular shifts in the resonance positions are plotted as a function of binding energy in Fig. 9. It can be seen that the calculated shifts agree reasonably well with those determined experimentally except for the deepest level, which is underestimated. Note, furthermore, that the asymmetric shape of the experimental resonances is reproduced in the calculation. This originates from the imaginary part in the integral (20), which is quite large for the graphite case.

These shifts in resonance positions are band-structure effects arising from the mixing of unperturbed states caused by the surface corrugation. If the corrugation is sufficiently small, the band gaps are given by second order perturbation theory as

$$\Delta_{ij} = \pm 2\langle \phi_i(z) | V_{\vec{G}}(z) | \phi_j(z) \rangle, \tag{22}$$

where ϕ_i is an eigenfunction of the Schrödinger

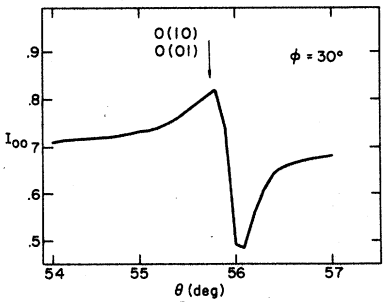

FIG. 8. Computed structure at $\phi = 30°$ associated with the crossing of 0(01) and 0(10) levels. Vertical bar denotes unperturbed resonance position.

equation for the potential $V_0(z)$. While this assignment cannot be made with the corrugated hard-wall potential (for which the matrix elements vanish), it can be evaluated from the more realistic pairwise sum potentials of Sec. III. The matrix elements are approximately proportional to the angular shifts shown in Fig. 9, according to the relation

$$\Delta_{ii} = \frac{2\hbar^2 k^2}{m} \Delta\Theta_{ii} \left[\sin\theta + \left(\frac{G_{01}\sqrt{3}}{2k} \right) \cos\theta \right].$$

While it appears that the data of Fig. 9 exhibit a nonzero limit as ϵ_j tends to zero, this is misleading. In particular, the normalization constant C of the wave function for a weakly bound state satisfies in the quasi-classical approximation[45]

$$2/C^2 \simeq \int \frac{dz}{p(z)}, \tag{23a}$$

$$2/C^2 = \frac{\hbar\pi}{m} \frac{\partial n(E)}{\partial E}, \tag{23b}$$

where the integral in Eq. (23a) is over the classically allowed domain of z. The derivative of quantum number with respect to energy can be evaluated[46,47] for long-range attractive potentials of the form $-C_3 z^{-3}$, yielding $\partial n/\partial E \propto |E|^{-5/6}$. The overlap integral of Eq. (22) will have only a weak dependence on energy, apart from a factor C^2, yielding $\Delta_{ii} \propto C^2 \propto |E|^{5/6}$. Thus the matrix element should indeed become small as $|E| \to 0$, because of the increasing spread of the wave function for large n. The discreteness of the spectrum, of course, could, in principle, preclude the existence of states satisfying this limiting behavior. Figure 9 indicates, however, that the argument is indeed relevant to the ^{4}He case.

The original work of Boato *et al.*[2] reported only four energy levels. The weak minimum labeled T in Fig. 3(a) was identified as a threshold effect in part because no splitting of that level was present in the data. As the preceding analysis indicates, this splitting is simply very small. Our calculations clearly indicate the presence of at least $n=4$ (which has recently been determined by Derry *et al.*) and $n=5$ eigenvalues. Figure 10 shows these resonances at $\phi = 0$.

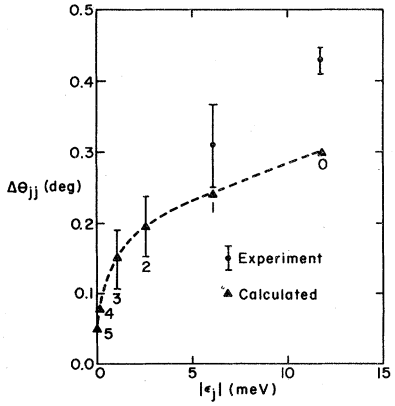

FIG. 9. Angular splittings between minimum positions for various levels j coupled by the lowest nonzero Fourier component of the potential, as a function of binding energy $|\epsilon_j|$.

V. CONCLUSIONS

We have found the corrugated hard wall plus attractive potential to represent rather well the scattering data of Boato *et al.*[2] for ^{4}He incident on basal plane graphite. The hard-wall corrugation has a range $\Delta z \simeq 0.21$ Å (maximum to minimum) which is intermediate between alkali-halide surfaces and compact metal surfaces. Its origin can be understood in terms of a pairwise summation of pair potentials $U(\vec{r} - \vec{R}_i)$. The He-C interaction $U(\vec{r} - \vec{R}_i)$ can be represented by either Yukawa-6 or Lennard-Jones 6-12 forms. In the latter case, our optimal parameters differ significantly from those employed in earlier studies of the He-graphite system[25] and give good agreement with recent thermodynamic measurements for both ^{3}He and ^{4}He.[6,7]

We have confirmed the prediction of our preliminary study[13] concerning the existence of the $n=4$ and 5 bound states. The behavior near threshold is particularly difficult to deduce from the experiment because the resonances tend to be smeared by both experimental problems and inelastic effects. The recent observation by Derry *et al.*[3] of the state $\epsilon_4 \simeq -0.2$ meV is consistent with our predictions.

Our study, following the method of Ref. 12, shows how the line shapes and splittings can be understood in terms of the phase-shift derivative $d\delta/d\epsilon$. The latter is especially appealing when analyzed using semiclassical theory because of its simplicity. In particular, these features permit

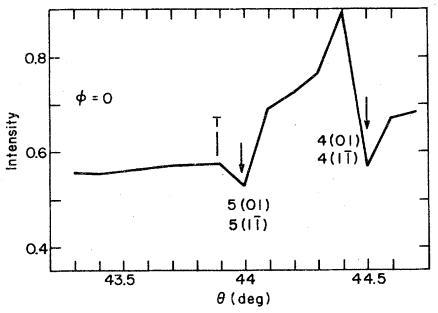

FIG. 10. Predicted specular intensity near threshold as a function of incident polar angle for $\phi = 0$.

deduction of relative linewidths from the bound-state resonance positions.

Inelastic effects seem to be important in this system. Our model calculation of their role is intended primarily as a stimulus to future analysis, using microscopic theory, of the loss processes. It is not certain whether the elastic or electronic properties of graphite provide the origin of the apparent inelastic scattering. Measurement of the final-state energy would help elucidate this situation.

Calculations are in progress of alternative model potential forms, band structure, and ^{3}He scattering. We intend also to examine the implications for thermodynamic measurements (both binding energy and heat capacity) of our results. This overlap of superficially disparate fields represents an exciting aspect of the He-graphite system.

Note added in proof. More recently we have found it necessary to include anisotropy in the He-C pair interaction. See W. E. Carlos and M. W. Cole, Phys. Rev. Lett. 43, 697 (1979).

ACKNOWLEDGMENTS

It is a pleasure to thank J. Hutchison, F. O. Goodman, G. Boato, P. Cantini, D. R. Frankl, G. Derry, and D. Wesner for assistance, stimulating discussion and communication of results prior to publication. One of us (N.G.) would like to thank the Department of Physics at the University of Virginia for financial support.

This work was supported in part by National Science Foundation grant DMR-76-17375 and by a research initiation grant from The Pennsylvania State University.

[1]For recent reviews, see F. O. Goodman, CRC Crit. Rev. Solid State Mater. Sci. 7, 33 (1977); and M. W. Cole and D. R. Frankl, Surf. Sci. 70, 585 (1978).

[2]G. Boato, P. Cantini, and R. Tatarek, Phys. Rev. Lett. 40, 887 (1978); G. Boato, P. Cantini, R. Tatarek, and G. P. Felcher, Surf. Sci. 80, 518 (1979).

[3]G. Derry, D. Wesner, W. E. Carlos, and D. R. Frankl, Surf. Sci. 87, 629 (1979).

[4]G. Boato, P. Cantini, C. Guidi, R. Tatarek, and G. P. Felcher, Phys. Rev. B 20, 3957 (1980).

[5]W. A. Steele, *The Interaction of Gases with Solid Surfaces* (Pergamon, Oxford, 1974); J. Phys. Chem. 82, 817 (1978).

[6]R. L. Elgin and D. L. Goodstein, Phys. Rev. A 9, 2657 (1974).

[7]R. L. Elgin, J. M. Greif, and D. L. Goodstein, Phys. Rev. Lett. 41, 1723 (1978).

[8]N. García, Phys. Rev. Lett. 37, 912 (1976); J. Chem. Phys. 67, 879 (1977).

[9]C. E. Harvie and J. H. Weare, Phys. Rev. Lett. 40, 187 (1978); K. Wolfe and J. H. Weare, Phys. Rev. Lett. 41, 1663 (1978); Solid State Commun. 27, 1293 (1978).

[10]N. García, V. Celli, and F. O. Goodman, Phys. Rev. B 19, 634 (1979); N. García, F. O. Goodman, V. Celli, and N. R. Hill, Phys. Rev. B (to be published).

[11]H. Chow and E. D. Thompson, Surf. Sci. 59, 225 (1976).

[12]V. Celli, N. García, and J. Hutchison, Surf. Sci. 87, 101 (1979).

[13]A preliminary investigation of the He–graphite potential was presented by W. E. Carlos and M. W. Cole, Surf. Sci. 77, L173 (1978).

[14]W. E. Carlos, G. Derry, and D. R. Frankl, Phys. Rev. B 19, 3258 (1979).

[15]N. Cabrera and J. Solana, in *Proceedings of the International School of Physics "Enrico Fermi,"* Course 58: edited by F. O. Goodman (Compositori, Bologna, 1974), p. 530; N. García, Surf. Sci. 71, 220 (1978).

[16]H. Chow, Surf. Sci. 79, 157 (1979); H. Chow and E. D. Thompson, *ibid.* 82, 1 (1979).

[17]The Rayleigh hypothesis is valid only for small values of the corrugation strength. See Refs. 18 and 19.

[18]N. R. Hill and V. Celli, Phys. Rev. B 17, 2478 (1978).

[19]N. García and N. Cabrera, Phys. Rev. B 18, 576 (1978); N. García, V. Celli, N. R. Hill, and N. Cabrera, Phys. Rev. B 18, 5184 (1978).

[20]A. M. Marvin and F. Toigo, Solid State Commun. 27, 233 (1978).

[21]D. L. Freeman, J. Chem. Phys. 62, 941 (1975).

[22]See Ref. 15 for further discussion.

[23]G. Boato and P. Cantini, private communication.

[24]See D. R. Hartree, *Calculations of Atomic Structures* (Wiley, London, 1957).

[25]D. E. Hagen, A. D. Novaco, and F. J. Milford, in *Adsorption-Desorption Phenomena,* edited by F. Ricca (Academic, London, 1972), p. 99; E. Giamello, C. Pisani, F. Ricca, and C. Roetti, Surf. Sci. 49, 401 (1975).

[26]K. M. Smith, A. M. Rules, G. Scoles, R. A. Aziz, and V. Nain, J. Chem. Phys. 67, 152 (1977).

[27]H. G. Drickamer, R. L. Clenenden, R. W. Lynch, and E. A. Perez-Albuerne, in *Solid State Physics,* edited by F. Seitz and D. Turnbull (Academic, New York, 1976), Vol. 19, p. 135.

[28]I. S. Gradshteyn and I. M. Ryzhik, *Tables of Integrals, Series and Products* (Academic, New York, 1965), p. 1972.

[29]R. G. Gordon and Y. S. Kim, J. Chem. Phys. 56, 3122 (1972).

[30]G. S. Painter and D. E. Ellis, Phys. Rev. B 1, 4747 (1970).

[31]H. Watanabe, private communication. Recently G. Vidali, M. W. Cole, and C. Schwartz, [Surf. Sci. (to be published)] obtained $C_3 = 186$ meV Å^3. Note that the z^{-3} behavior must be modified in the very-large-z limit where retardation enters.

[32]G. G. Kleiman and U. Landman, Phys. Rev. B 8, 5484 (1973); E. Zaremba and W. Kohn, Phys. Rev. B 15, 1769 (1977). The $z = 0$ plane is defined there to eliminate a z^{-4} term in the series expansion of the dispersion.

[33]U. Garibaldi, A. C. Levi, R. Spadacini, and G. E.

Tommei, Surf. Sci. 48, 699 (1975).
[34]N. García, G. Armand, and J. Lapujoulade, Surf. Sci. 68, 399 (1977).
[35]M. W. Cole and M. Schmeits, Surf. Sci. 75, 529 (1978).
[36]See F. O. Goodman, Surf. Sci. 65, 37 (1977); and Ref. 1.
[37]S. V. Krishnaswamy, G. Derry, D. Wesner, T. J. O'Gorman, and D. R. Frankl, Surf. Sci. 77, 493 (1978).
[38]N. García and V. Celli, Surf. Sci. (to be published).
[39]B. F. Mason and B. R. Williams, Surf. Sci. 75, L786 (1978).
[40]J. Lapujoulade and Y. Lejay, European Physical Conference, York, England, September, 1978 (unpublished); and private communication.
[41]K. Komatsu, J. Phys. Chem. Solids 6, 380 (1958).
[42]E. Müller-Hartmann, T. V. Ramakrishnan, and G. Toulouse, Solid State Commun. 9, 99 (1971).
[43]This is probably naive. See e.g., P. M. Echenique and J. B. Pendry, J. Phys. C (Solid State) 9, 3183 (1976), who explored the case of scattering by a liquid surface.
[44]H. Chow, Surf. Sci. 66, 22 (1977).
[45]L. D. Landau and E. M. Lifshitz, *Quantum Mechanics* (Pergamon, London, 1958), Sec. 47.
[46]R. J. Le Roy, Surf. Sci. 59, 541 (1976).
[47]M. W. Cole and T. T. Tsong, Surf. Sci. 69, 325 (1977).